Kenalog modified by ionizing radiation induces intrinsic apoptosis mediated by elevated levels of reactive oxygen species in melanoma cancer

REMIGIUS AMBROSE KAWALA[1,2], FATUMA JUMAPILI RAMADHANI[1,2], HYO JIN CHOI[1], EUN-HEE LEE[1], CHUL-HONG PARK[1], BYUNG YEOUP CHUNG[1] and HYOUNG-WOO BAI[1,2]

[1]Advanced Radiation Technology Institute (ARTI), Korea Atomic Energy Research Institute (KAERI), Jeongeup-si, Jeollabuk-do 580-185; [2]Radiation Biotechnology and Applied Radioisotope Science, University of Science and Technology (UST), Daejeon 34113, Republic of Korea

Received June 16, 2018; Accepted December 6, 2018

DOI: 10.3892/or.2018.6940

Abstract. Kenalog is a synthetic glucocorticoid drug used to treat various cancers including ocular and choroidal melanoma. However, the drug achieves rarely sustainable results for patients. To overcome this difficulty, the structure of Kenalog was altered by ionizing radiation (IR) to develop a more effective anticancer agent for treatment of various skin cancers. The anticancer effect of modified Kenalog (Kenalog-IR) was assessed in melanoma cancer cells *in vitro*. The assessment of mitochondrial functions by MTT assay revealed significant inhibition of melanoma cancer cell viability by Kenalog-IR compared to Kenalog. Moreover, Kenalog-IR-induced apoptotic cell death was associated with the intrinsic mitochondrial pathway by triggering the release of intrinsic apoptosis molecules through activation of caspase-related molecules in concentration and time-dependent manners. Furthermore, it was observed that Kenalog-IR-induced apoptosis was associated with the generation of reactive oxygen species (ROS) with increased G2/M cell cycle arrest. Collectively, Kenalog-IR may be a potential suppressor of skin-related cancer in particular melanoma cancer.

Correspondence to: Dr Hyoung-Woo Bai, Advanced Radiation Technology Institute (ARTI), Korea Atomic Energy Research Institute (KAERI), 29 Geumgu-gil, Jeongeup-si, Jeollabuk-do 580-185, Republic of Korea
E-mail: hbai@kaeri.re.kr

Abbreviations: IR, ionizing radiation; MTT, 3-(4,5-dimethylthiazol-2-yl)-2,5-diphenyltetrazolium bromide; ROS, reactive oxygen species; IMD, incrementally modified drugs

Key words: Kenalog, Kenalog-IR, ionizing radiation, melanoma cancer, apoptosis and ROS

Introduction

Glucocorticoids have been used for the treatment of various disorders including skin-related diseases and cancers (1,2) and in recent years, several trials have been performed to assess their use as adjuvant therapy in various applications (2-4). They have inhibitory effects in choroidal neovascularization and were revealed to be generally effective in providing anti-inflammatory effects and short-term relief in mice (5). Kenalog (triamcinolone acetonide), a synthetic glucocorticoid is commonly used to treat various diseases such as ocular and choroidal melanoma (6,7). However, like many other glucocorticoids, treatment with Kenalog aggravates side effects and rarely achieves sustainable results for patients and in cases requiring chronic therapy (8,9). This may be due to the ability of some tissues such as skin cells including melanoma to produce glucocorticoids from cholesterol due to intramolecular rearrangements caused by UV light that may impair the effectiveness of the drug (10,11).

In recent years, several approaches have been devised to increase the bioactivity of glucocorticoids to overcome the problems related to low efficacy and increased adverse effects (12). One of the approaches is incrementally modified drugs (IMD) (13). IMD involves the addition of functional groups and/or synthesis of a conventional drug chemically. Using this innovative technology, several modified glucocorticoid drugs, for example nitro-steroids 21-NO-prednisolone and many other NO-releasing nonsteroidal anti-inflammatory drugs (NSAIDs), have been demonstrated to have enhanced efficacy (14). However, efforts made thus far in IMD do not cater enough to the use of physical means such as ionizing radiation (IR). With this in mind, the use of ionizing radiation was developed to improve the potency and efficacy of glucocorticoids in cancer treatment. Various studies have reported the use of ionizing radiation to improve the efficacy of glucocorticoids (15). In a previous study, we revealed that rotenone derivatives modified by ionizing radiation had potential anti-carcinogenic activity in hepatic cancer cells (16). The aim of the present study, was to further improve our knowledge on γ-irradiated glucocorticoids as potential anticancer drugs for

the treatment of various types of cancer. In the present study, Kenalog-IR was reported as a potential candidate for the treatment of skin cancer.

To elucidate the contribution of IR in IMD approaches, the *in vitro* cytotoxic effects of Kenalog-IR were assessed in melanoma cancer cells. It was found that Kenalog-IR generated more effective anticancer activity when compared to Kenalog and was confirmed as a suitable candidate for cancer treatment. The present results revealed that the induction of the intrinsic apoptosis pathway was associated with the production of ROS and exhibited anticancer activity potential and the results were in line with a previous study which revealed γ-radiation-modified dexamethasone as a potential target in human lung cancer treatment (17). Although, the structure of Kenalog-IR remains to be determined, its potential anticancer activity cannot be ruled out for the treatment of melanoma skin cancer.

Materials and methods

Preparation of Kenalog suspension and irradiation. The Kenalog drug was obtained from Sigma-Aldrich; Merck KGaA (Darmstadt, Germany) and 1 g of the stock was dissolved in a liter of methanol. The suspension was irradiated at 50 kGy at a dose rate of 10 kGy/h generated by a ^{60}Co irradiator (MDS Nordion, Ottawa, ON, Canada) at the Advanced Radiation Technology Institute, Korea Atomic Energy Research Institute. Irradiated samples were evaporated *in vacuo*, and crude compounds were analyzed by liquid chromatography coupled with mass spectrometry (LC-MS) and liquid chromatography (HPLC). To determine the chromatograms of the Kenalog-IR, irradiated samples were evaporated *in vacuo* and analyzed by high performance HPLC or LC-MS (Agilent Technologies, Inc., Palo Alto, CA, USA) in a YMC-Pack ODS-A-302 column (4.6 mm i.d. x 150 mm; YMC Co., Ltd., Kyoto, Japan). The mobile phase comprised of linear gradient starting with 0.1% (v/v) HCOOH at 40˚C and increased to 50% (v/v) MeCN in 0.1% (v/v) CHOOH/H_2O over 20 min, and then increased to 100% MeCN for a further 20 min (detection, UV 254 nm; flow rate, 1.0 ml/min). This irradiated solution was named Kenalog-IR and a final concentration of 1 mg/ml was used for analysis.

Cell culture. The cell lines used for the present study, SK-Mel-5 was purchased from the American Type Culture Collection (ATCC; Rockville, MD, USA) and CCD-986sk skin fibroblast was obtained from the Korean Cell Line Bank (KCLB; Seoul, Korea). SK-Mel-5 cells were prepared in Dulbecco's modified Eagle's medium (DMEM) and CCD-986sk in Roswell Park Memorial Institute (RPMI)-1640 medium with 100 U/ml penicillin and 100 μg/ml streptomycin and 10% heat-inactivated fetal bovine serum (FBS) (Gibco; Thermo Fisher Scientific, Inc., Waltham, MA, USA). Cells were maintained at 37˚C, in an incubator until 80-90% confluence was reached, and an equal number of cells were incubated without or with various concentrations of Kenalog and Kenalog-IR (0, 5, 10, 25, 50 and 100 μg/ml) for each set of experimental conditions. Cells were washed with 1X phosphate-buffered saline pH 7.4 (PBS) and harvested with 0.5% trypsin-0.2% EDTA (Gibco; Thermo Fisher Scientific, Inc.) and were either used directly for analysis or stored at -80˚C for further analysis.

Cell viability and proliferation. Cell viability was measured by determining mitochondrial function using MTT assay kit [3-(4,5-dimethylthiazol-2-yl)-2,5-diphenyltetrazolium bromide (Roche Diagnostics, Indianapolis, IN, USA)] and cell toxicity was assessed by trypan blue staining. The SK-Mel-5 cells were seeded at a density of $0.3x10^4$ cells/well in a 96-well flat bottom plate. After 24 h, the cells were treated with various concentrations of Kenalog or Kenalog-IR for 24 and 48 h. After treatment, 20 μl of 5 mg/ml MTT solution was added to each well and incubated for 2.5 h at 37˚C, in a 5% CO_2 atmosphere. The supernatant was removed and solubilized with dimethyl sulfoxide (DMSO) for 10 min to dissolve the formazan produced. The absorbance was measured at 570 nm using a microplate reader (Tecan Group Ltd., Männedorf, Switzerland). Cell viability was expressed as the percentage of difference from the control at the corresponding concentration points. For the cytotoxic (cell death) assay, the cells were treated with various concentrations of compounds as aforementioned at a density of $0.3x10^6$ in a 65-mm culture dish. The staining was carried out by trypan blue dye-exclusion using a counting chamber and dead and live cells were counted by an Olympus IX71fluorescence microscope (Olympus Corp., Tokyo, Japan). To assess the non-specific cytotoxic effect of Kenalog-IR, normal skin fibroblast cells CCD-986sk were used. Briefly, $0.3x10^6$ cells/well were seeded into a 96-well plate for 96 h and subsequently treated with Kenalog or Kenalog-IR for 24 and 48 h. Then, cell viability was assessed by MTT assay as aforementioned.

Apoptotic assay determination. For quantitative analysis of apoptotic and necrotic dead cells, Muse Annexin V and Dead Cell Assay kit (MCH100105; EMD Millipore, Billerica, MA, USA) was used. SK-Mel-5 cells ($3x10^5$) were seeded in a 65-mm culture dish for 24 h and then treated with 100 μg/ml of Kenalog or Kenalog-IR for 24 h at 37˚C, in a 5% CO_2 atmosphere. Cells were harvested and washed with PBS pH 7.4 as aforementioned. Furthermore, the cells were stained with Annexin V and Dead Cell reagent for 20 min and flow cytometric assessment was performed by Muse™ Cell Analyzer (EMD Millipore). The live and apoptotic cells were distinguished from necrotic cells as follows: Live cells (Annexin V-FITC$^-$/PI$^-$) called double negative, early apoptotic cells (Annexin V-FITC$^+$/PI$^-$), late apoptotic cells (Annexin V-FITC$^+$/PI$^+$) called double positive and necrotic cells (Annexin V-FITC$^-$/PI$^+$). The apoptotic cells were expressed as the percentage of live cells, early/late apoptotic cells, and dead cells determined by Muse analysis software (Muse 1.1.2; EMD Millipore).

Determination of DNA fragmentation. The chromosomal DNA fragments were identified using agarose gel electrophoresis. Briefly, $3x10^5$ SK-Mel-5 cells were seeded and treated with 100 μg/ml Kenalog or Kenalog-IR and 2 μM doxorubicin for 18 h. The 0.1% DMSO contained media and the fresh media-treated cells were used as vehicle and control, respectively. After treatment, the cells were washed two times with PBS and cell lysates were harvested by DNA lysis buffer-1 (10 mM EDTA, 0.25% Triton X-100 and 2.5 mM Tris-HCl

at pH 8) and incubated at room temperature (RT) for 15 min. Cells were centrifuged at 13,000 x g for 20 min at 4˚C and an equal volume of supernatant and isopropanol were mixed and incubated at -80˚C for 1 h. After cold incubation, the samples were centrifuged at 13,000 x g for 20 min at 4˚C and the pellets were washed three times with cold 75% ethanol by centrifugation at 13,000 x g for 20 min at 4˚C. Pellets were then left to dry at RT and suspended with 100 μl of DNA lysis buffer-2 (10 mM EDTA, and 2.5 mM Tris-HCl at pH 8). The samples were further incubated with 0.1 mg/ml RNase A for 30 min at RT and mixed with 0.25 mg/ml proteinase K for 1 h at RT. Then, the samples were mixed with 6X loading dye to a final concentration of 1X, and loaded in 1.2% agarose gel containing 1X gel red stain. Electrophoresis was run for 30 min at 100 V/cm.

Cell cycle assessment. For cell cycle assessment, Muse cell cycle reagent (EMD Millipore) was used. The analysis of differential DNA content in each phase of the cell cycle (G0/G1, S, and G2/M) was determined in melanoma cells. Briefly, $3x10^5$ SK-Mel-5 cells were seeded and treatment was carried out as described in the apoptosis assay aforementioned. Nocodazole (400 nM) was used to induce G2/M phase cell arrest. Cells were then stained and incubated for 30 min with Muse cell cycle reagent at 4˚C and flow cytometric assessment was performed by Muse™ Cell Analyzer (EMD Millipore). The DNA content was expressed as the percentage of cells in the respective cell cycle phase.

Assessment of reactive oxygen species (ROS). Intracellular ROS produced by stressed cells were assessed by Muse oxidative stress reagent assay (EMD Millipore). SK-Mel-5 cells ($1x10^5$) were seeded in a 65-mm culture dish for 24 h and then treated with 100 μg/ml of Kenalog and Kenalog-IR or 2 μM doxorubicin as the positive control. Cells were harvested and the cell suspension was incubated with assay reagent for 30 min and the oxidized red dihydroethidium (DHE) fluorescence intensity was assessed by flow cytometer using Muse™ Cell Analyzer (EMD Millipore). The ROS-positive and ROS-negative cells were expressed as a percentage of the ROS gated profile. For the intracellular source of ROS determination, MitoSOX assay (Invitrogen; Thermo Fisher Scientific, Inc.) was used. Cells were pre-labeled with MitoSOX reagent before treatment. Then cells were treated as indicated above for 18 h and harvested with trypsin. The cells were harvested, washed and further incubated with a buffer containing 5 μM MitoSOX for 10 min at 37˚C in the dark. After the incubation time, the cells were washed twice and suspended for measurements with a flow cytometer.

Western blot analysis. Treated and untreated SK-Mel-5 cells were harvested, lysed with radioimmunoprecipitation assay buffer (RIPA; Rockland Immunochemicals, Inc., Limerick, PA, USA) and cytosolic and mitochondria fractions were separated by Cytochrome *c* Release Apoptosis Assay kit (cat. no. ab65311; Abcam, Cambridge, UK) following the manufacturer's instructions. Cell debris was removed by centrifugation and the protein concentration was determined by bicinchoninic acid protein assay kit (Thermo Fisher Scientific, Inc.) according to the manufacturer's instructions. Cell lysates containing an equal amount of protein (40 μg) were prepared and separated by 10 or 15% SDS-PAGE and 10 μg of cytosolic fractions and 15 μg of both mitochondria and debris fractions were loaded onto 12% SDS-PAGE and transferred to polyvinylidene difluoride membranes (PVDF; Merck Millipore). The membranes were then blocked with 5% non-fat milk in Tris-buffered saline containing Tween-20 (TBST) for 1 h at RT. The membranes were subsequently probed overnight at 4˚C with primary antibodies at dilution of 1:1,000 for anti-Bcl-2 (cat. no. 2870), anti-Bax (cat. no. 5023), anti-Bad (cat. no. 9292), anti-caspase-9 and cleaved caspase-9 (cat. no. 9502), anti-caspase-7 (cat. no. 9492) and cleaved caspase-7 (cat. no. 9491), anti-caspase-3 (cat. no. 9662) and cleaved caspase-3 (cat. no. 9664), anti-PARP (cat. no. 9532) and cleaved PARP (cat. no. 9541), anti-AIF, anti-AKT (cat. no. 4691) and p-AKT (cat. no. 4060), anti-mTOR (cat. no. 2983) and p-mTOR (cat. no. 5536), anti-β-actin (cat. no. 4970) and anti-GAPDH (cat. no. 2118) (all primary antibodies; Cell Signaling Technology, Danvers, MA, USA) and sodium dismutase-1 (cat. no. SC-11407) (Santa Cruz Biotechnology, Santa Cruz, CA, USA). The blots were then incubated with secondary antibody horseradish peroxidase (HRP)-conjugated anti-mouse (cat. no. 7076 at 1:2,500) or anti-rabbit IgG (cat. no. 7074 at 1:3,000) both from Cell Signaling Technology (Danvers, MA, USA) for 1 h at RT. The membranes were incubated with the chemiluminescence (ECL) reagent (Thermo Fisher Scientific, Inc.) for protein band detection.

Statistical analysis. All data were evaluated by one-way ANOVA, followed by Tukey's post hoc test and results were considered statistically significant when the P-value was <0.05. Experiments were performed at least of three times independently.

Results

Effects of ionizing radiation on Kenalog. To investigate the radiolytic effects of ionizing radiation on Kenalog, 50 kGy of γ radiation was used to modify the chemical structures of the drug. Sample solutions of Kenalog and Kenalog-IR were analyzed by LC-MS and as revealed in Fig. 1, one major peak was observed in the chromatogram of Kenalog (Fig. 1, upper panel) and four peaks in the Kenalog-IR chromatogram at a various retention times (Fig. 1, lower panel). These newly generated peaks indicated that ionizing radiation caused alterations to Kenalog and that the changes may contribute to the cytotoxic effects of Kenalog-IR.

Kenalog-IR inhibits proliferation and induces cytotoxic effects in SK-Mel 5 cells. In order to investigate the anticancer activity of Kenalog-IR, MTT and trypan blue assays were used to evaluate the cytotoxic effects in the SK-Mel-5 cell line. It has been previously reported that the clinically available form of Kenalog has less cytotoxic effects compared to other corticosteroids (9). Thus, we first compared the cytotoxic effect of Kenalog and Kenalog-IR. As anticipated, Kenalog-treated cells exhibited a lesser effect on the viability of SK-Mel-5 cells in a concentration and time-dependent manner compared to Kenalog-IR. At 24 and 48 h, 100 μg/ml Kenalog-IR significantly reduced cell viability to 29% ($P=1x10^{-11}$) and

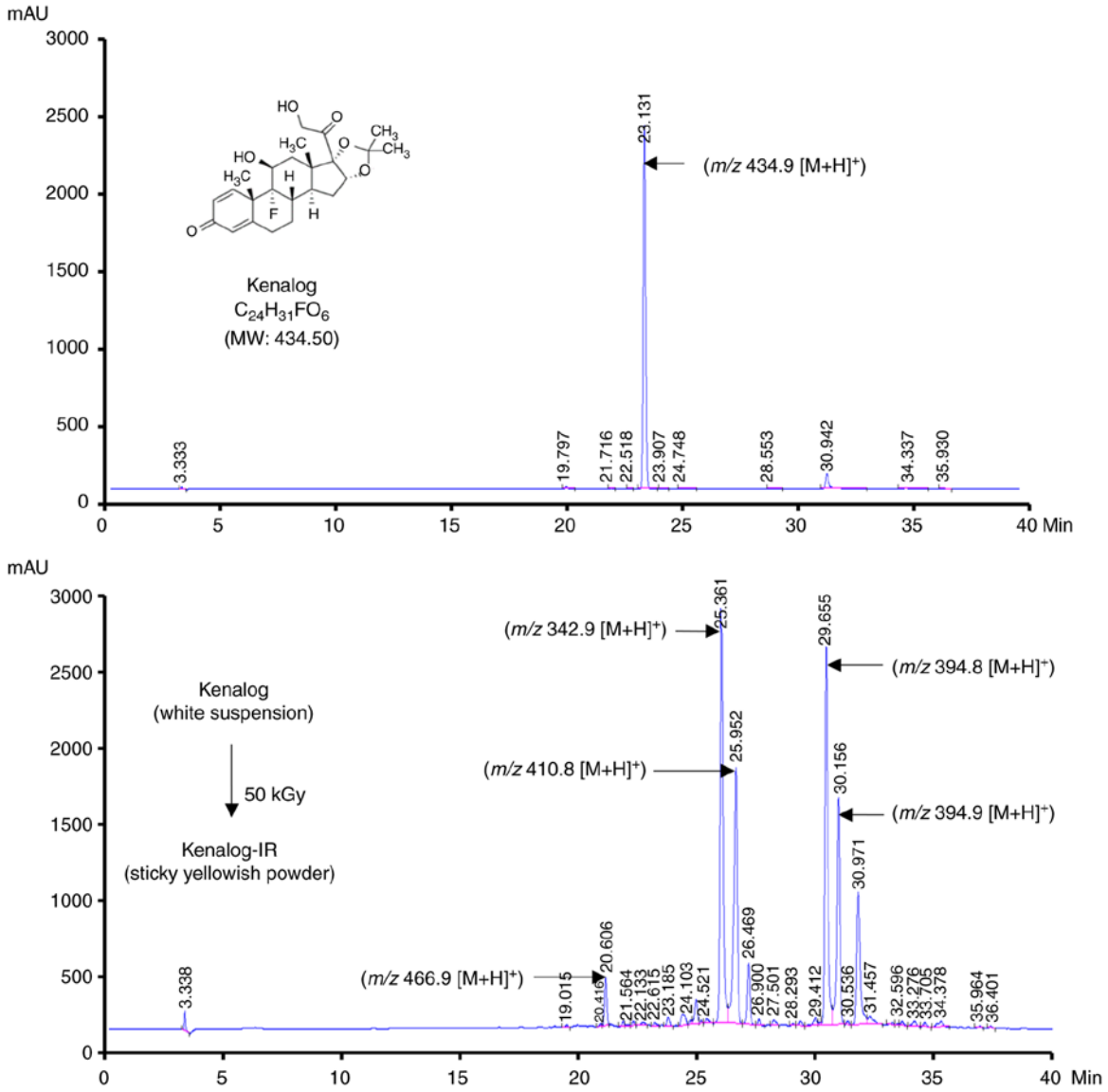

Figure 1. Effects of ionizing radiation on Kenalog. The chromatograms of Kenalog (upper panel) and Kenalog-IR (lower panel) of crude fractions. Kenalog (1 g) was dissolved in a liter of methanol and subjected to γ irradiation of 50 kGy. The white powder suspension changed to a yellow syrup after irradiation and exhibited four major peaks of Kenalog-IR at different retention times (lower panel) and one peak of Kenalog (upper panel) as assessed by LC-MS and HPLC. The arrows indicate the retention time of each peak. IR, ionizing radiation; LC-MS, liquid chromatography coupled with mass spectrometry; HPLC, liquid chromatography.

35% ($P=2x10^{-10}$), respectively (Fig. 2A) compared to the control and 100 μg/ml of Kenalog. In addition to the enhanced specific desired cytotoxic effect of the drug, attaining a platform that will not induce toxic effects in normal cells is very important in cancer treatment. The non-specific cytotoxic effects of Kenalog-IR in the skin fibroblast cell line CCD-986sk was observed. At 24 h, Kenalog-IR significantly reduced cell viability to 86% (P=0.004) but no significant differences (P=0.87) were observed between Kenalog and Kenalog-IR-treated groups (Fig. 2B). This indicated that treatment of SK-Mel-5 cells with Kenalog-IR induced less toxicity to normal cells. Furthermore, trypan blue assay also revealed that Kenalog-IR significantly induced 79% ($P=6x10^{-7}$) of cell death as compared to 8% (P=0.01) observed in Kenalog-treated cells (Fig. 2C). For the total number of cells, a similar trend was observed where Kenalog-IR reduced the number of cells to approximately half (Fig. 2D) when compared to the control and Kenalog-treated cells. In addition, the cytotoxic effects related to apoptosis were also observed by morphological changes in Kenalog-IR-treated cells. The morphological assessment revealed that, 100 μg/ml of Kenalog-IR caused plasma membrane protrusion and changes in pigmentation as observed with white patches (Fig. 2E). Collectively the results revealed that Kenalog-IR exhibited a potential effect in anticancer treatment compared to the original drug, Kenalog.

Kenalog-IR induces apoptosis and aggravates DNA integrity. As observed in Fig. 2, Kenalog-IR treated cells exhibited morphological changes and cell death when compared to Kenalog-treated cells. To understand the nature of Kenalog-IR-induced cell death, apoptosis and the cell cycle were assessed in SK-Mel-5 cells for 24 h. As indicated by flow cytometry, Kenalog-IR treated cells resulted in 62% ($P=2.5x10^{-12}$) of total apoptosis and 37% ($P=1.6x10^{-12}$)

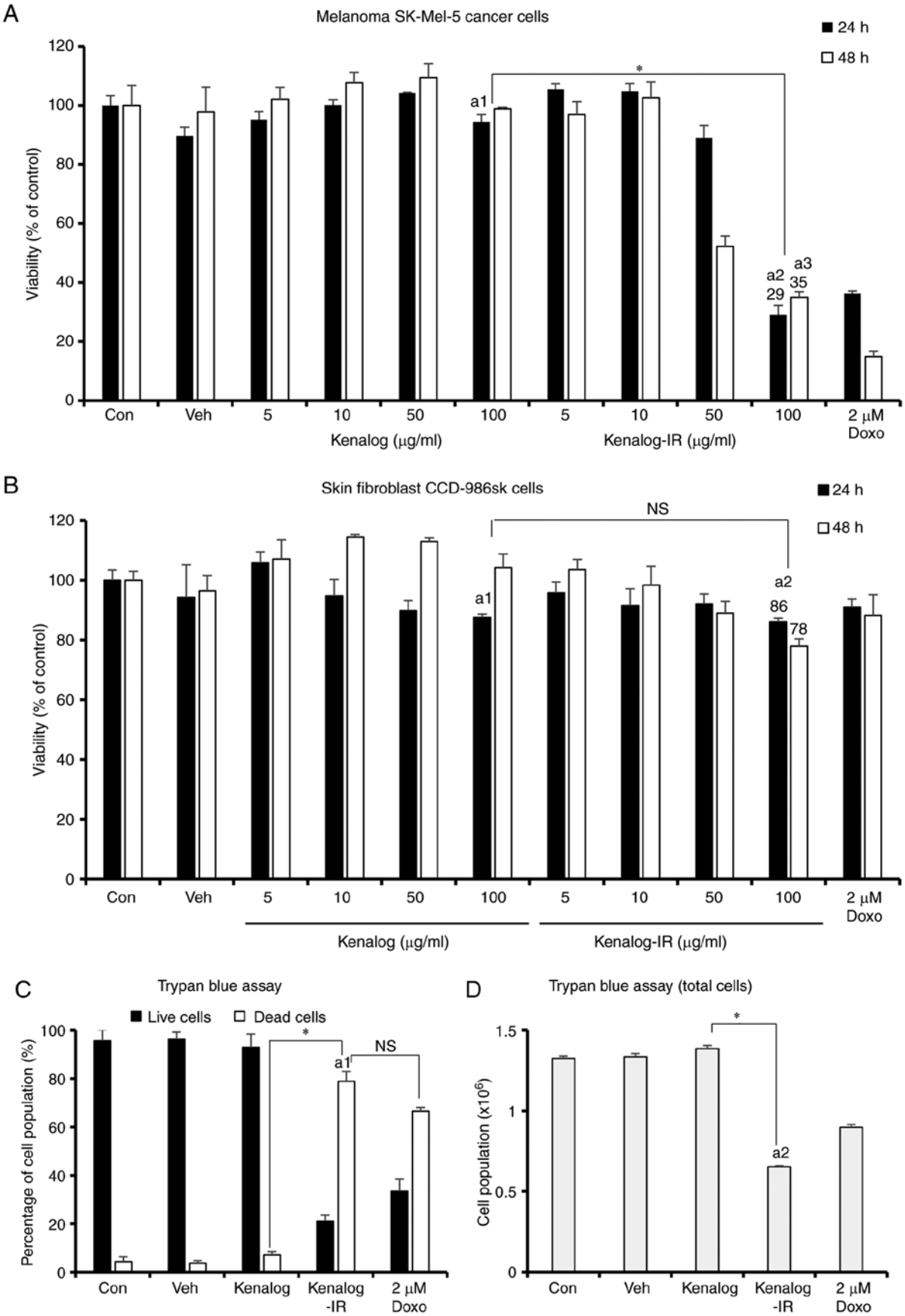

Figure 2. Kenalog-IR inhibits proliferation and induces cytotoxic effects in SK-Mel-5 cells. Cell viability and cell death of Kenalog and Kenalog-IR-treated cells. The viability of cells was assessed by MTT assay and was observed to be (A) decreased in a dose-dependent manner both at 24 and 48 h following Kenalog-IR treatment in SK-Mel-5 cells (^{a1}=0.003, ^{a2}=1x10^{-11}, ^{a3}=2x10^{-10}, *=1.1x10^{-9} at 24 h) and (B) less decreased in normal skin fibroblast cells, CCD-986sk (^{a1}=0.0004, ^{a2}=0.0004, $^{n.s}$=0.87). (C) Cell proliferation was determined by trypan blue exclusion assay. SK-Mel-5 cells were treated with 100 μg/ml of Kenalog and Kenalog-IR for 24 h (^{a1}=6x10^{-6}, *=0.01 and $^{n.s}$=0.251). (D) Indicates the reduction of the total number of cells (^{a2}=8.8x10^{-6} and *=0.01). A greater number of dead cells was observed in Kenalog-IR treated group.

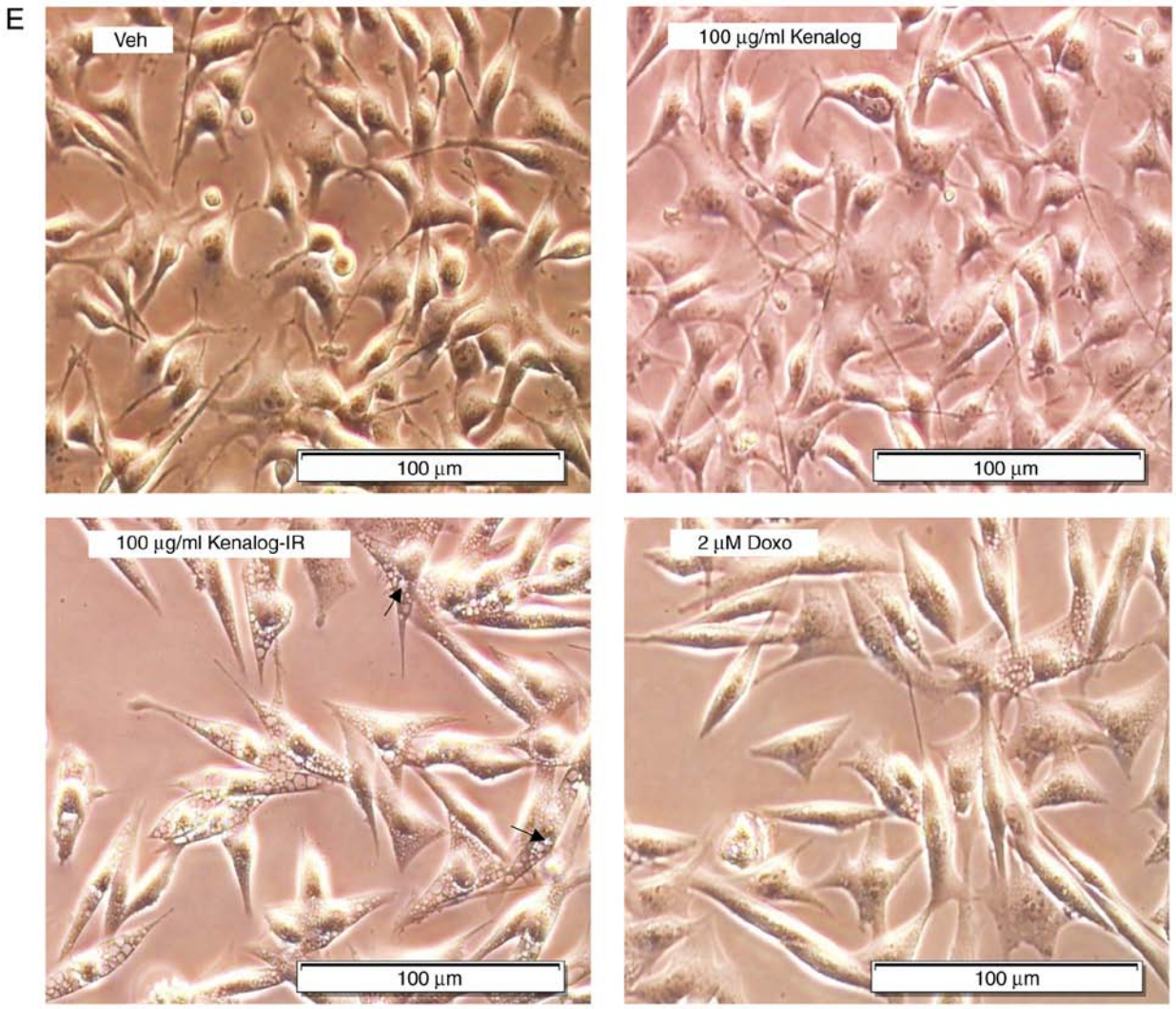

Figure 2. Continued. (E) Morphological appearance SK-Mel-5 following Kenalog and Kenalog-IR treatment for 24 h observed under a microscope. The arrows reveal white patches. Data are represented as the mean ± SEM of three independent experiments (*P<0.05 between treatment groups, 'NS' indicates not significant between treatment groups and a small letter 'a' indicates a significant difference between treatments and the control). IR, ionizing radiation.

of live cells (Fig. 3A and B). In comparison to the live cells in the control group, the reduction of a number of live cells in Kenalog-IR treated cells indicated that at 24 h many cells had progressed into apoptosis. Since apoptosis is known to be triggered through the intrinsic (caspase-mediated) pathway or extrinsic (death receptor-mediated) pathway, it was of interest to determine which pathway was involved in Kenalog-IR-induced cell death. To investigate this phenomenon, we blocked the intrinsic apoptosis pathway with caspase pan-inhibitor Z-VAD FMK and treated the cells as aforementioned. The results revealed that blocking caspase activation decreased total apoptosis to 28% ($P=1.09x10^{-5}$) in Kenalog-IR-treated cells (Fig. 3C and D) which indicated the involvement of intrinsic apoptosis in cell death. Furthermore, DNA fragmentation analysis revealed that Kenalog-IR induced cell death as confirmed by DNA fragments observed in a gel electrophoresis result (Fig. 3E, lane 5). To assess that no extrinsic apoptosis was involved, we investigated caspase-8, a key molecule in the extrinsic pathway. The result revealed no activation of caspase-8 in Kenalog-IR treated cells (Fig. 3F). Furthermore, it was of interest to reveal whether Kenalog-IR-induced apoptosis was related to cell cycle arrest. As revealed (Fig. 3G and H), Kenalog-IR induced 36.3% (P=0.003) cell arrest in the G2/M phase even when combined with nocodazole a known inducer of G2/M arrest, the same effect was observed (38.6%, $P=2.5x10^{-4}$). In sum, these data indicated that Kenalog-IR induced intrinsic apoptosis with a compromised cell cycle.

Kenalog-IR induces apoptosis through the intrinsic mitochondrial pathway. To further examine the apoptosis pathway involved in Kenalog-IR-induced cell death, the expression of several programmed cell death markers was examined by immunoblotting. Apoptosis is induced either by the intrinsic pathway based on caspase activation or the extrinsic pathways involving death receptors (18). The expression of pro- and anti-Bcl-2 family proteins, caspase-3 and PARP was gradually determined at 100 μg/ml (Fig. 4A). Further analysis of the Bcl-2 family 24 h after Kenalog-IR treatment, revealed increased levels of pro-apoptotic members Bax (P=0.0042) and Bad ($P=4x10^{-8}$) and decreased expression levels of anti-apoptotic member Bcl-2 (P=0.041) (Fig. 4B).

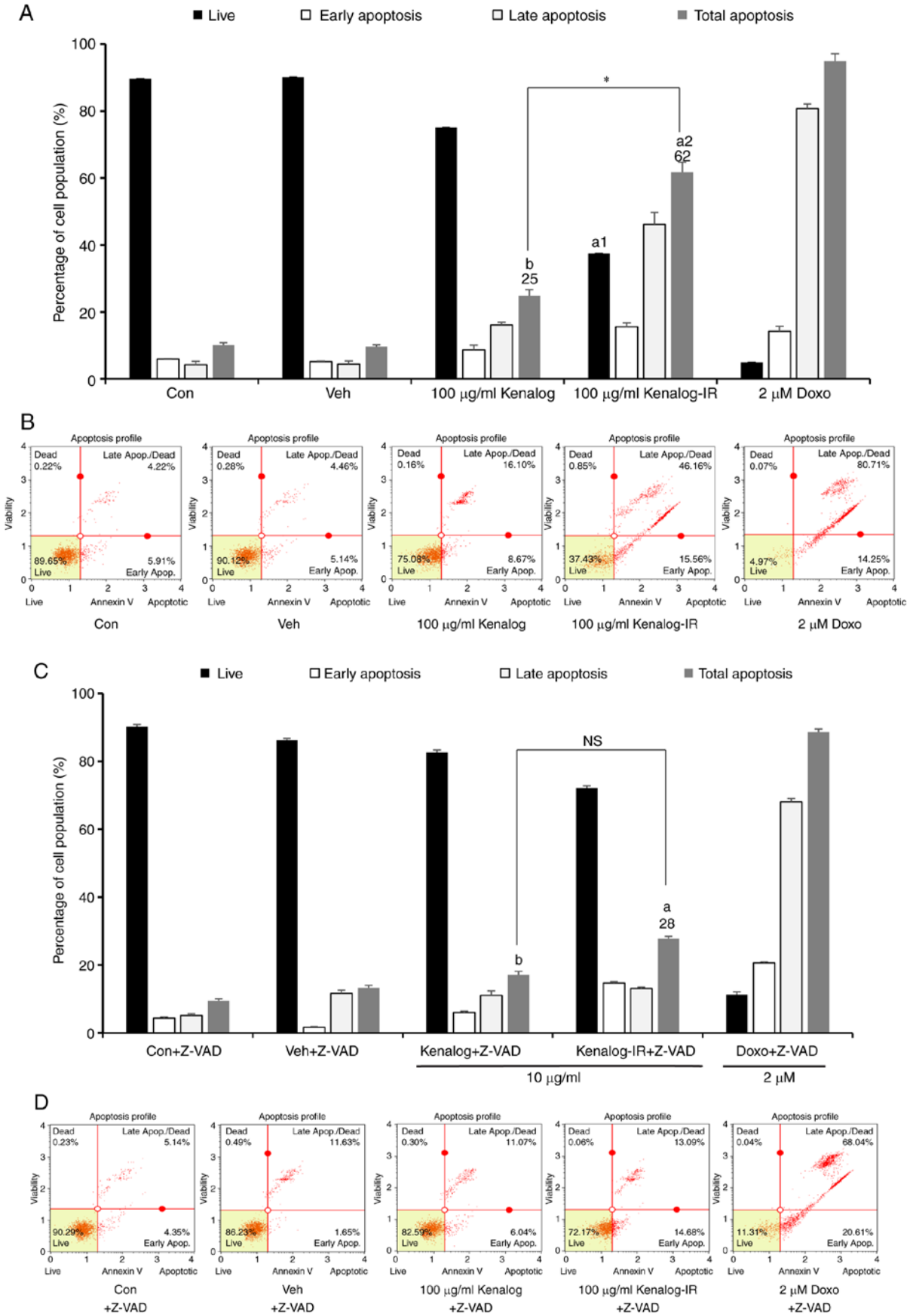

Figure 3. Kenalog-IR induces apoptosis with aggravating DNA integrity. Apoptosis and cell cycle analysis of Kenalog- and Kenalog-IR-treated cells was determined by Muse Annexin V-FITC/PI and a Muse cell cycle flow cytometer. (A) Percentage of live, early, late and total apoptosis. The population of positively stained propidium iodine cells was used to calculate the percentage of viable cells (^{a1}=2.5x10^{-12}, ^{a2}=1.6x10^{-12}, ^{b}=0.9, *=2.5x10^{-11}). (B) Quadrants indicating Annexin V-FITC/PI stained SK-Mel-5 cells exhibiting live, early apoptosis, late apoptosis, and dead cells. (C and D) Cells were pretreated with 40 μM of Z-VAD-FMK for 1 h and further treated with treatments + Z-VAD-FMK for 24 h. (C) Cells were harvested for percentage apoptosis analysis (^{a}=1.09x10^{-5}, ^{b}=0.84 and $^{n.s}$=0.73) and (D) Annexin V-FITC/PI quadrants.

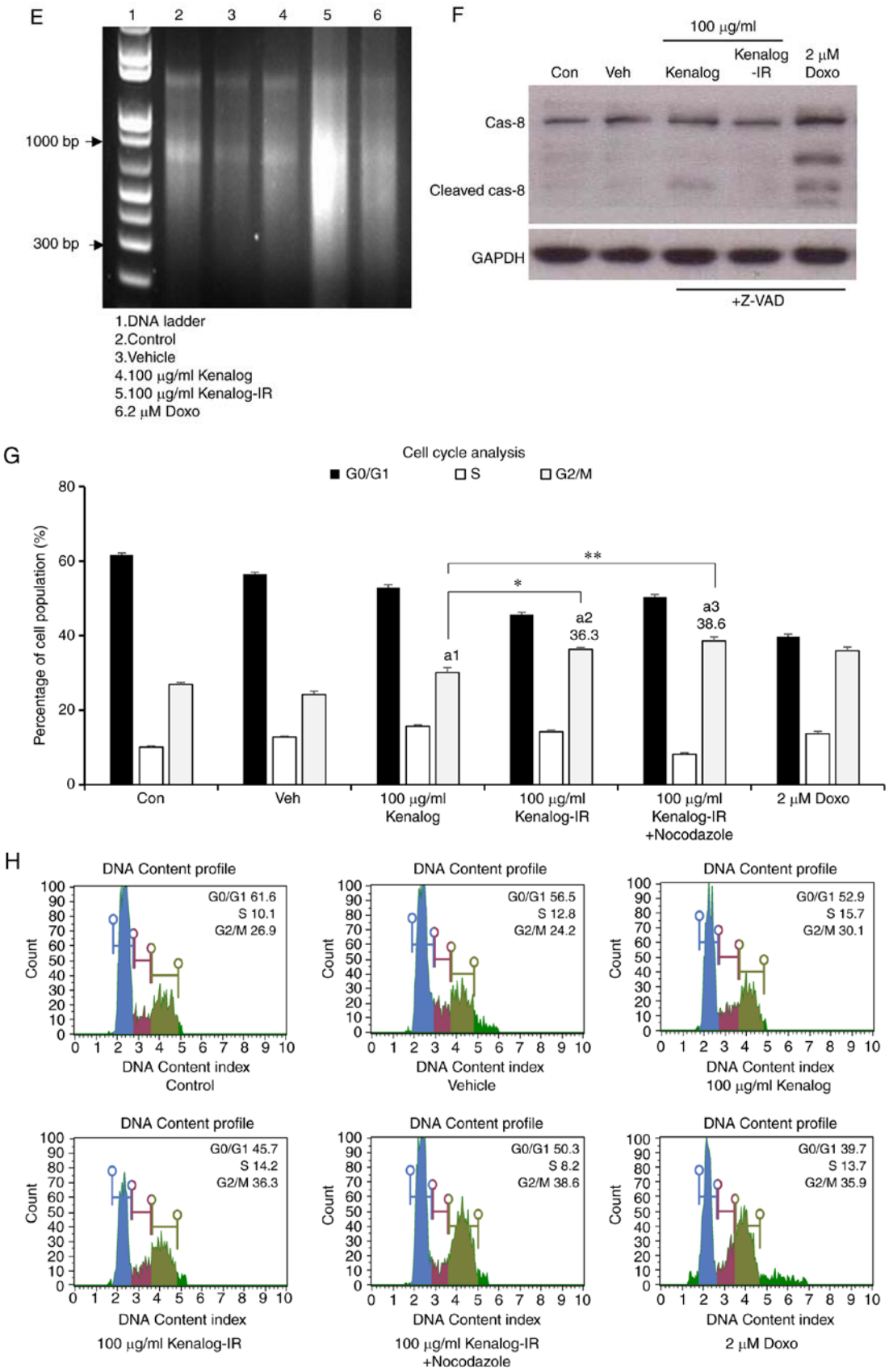

Figure 3. Continued. (E) DNA fragmentation assay. Cells were treated with treatments as indicated for 24 h and DNA was harvested for 1.2% gel electrophoresis. In addition, a DNA ladder (1 Kb) was used as the marker at 100 V/cm for 30 min. (F) Verification of extrinsic apoptosis. Cells were treated as indicated with Z-VAD-FMK for western blot assay. The anti-caspase-8 antibody was used to detect the extrinsic apoptosis pathway and GAPDH was used as a control. (G and H) Cell cycle analysis after 24 h of treatment. Nocodazole (400 nM) was used to induce G2/M cell cycle arrest. (G) The cell cycle summary (^{a1}=0.01, ^{a2}=0.003, ^{a3}=2.5x10^{-6}, *=1.8x10^{-5}, **=1.3x10^{-7}), and the phases indicated (H) the DNA content index profiles in each group and cell cycle phases G1/0, S and G2/M, expressed as the percentage of positively-stained cells (G). Data are presented as the mean ± SEM of three independent experiments (*P<0.05 between treatment groups, 'NS' indicates not significant between treatment groups, small letters 'a' and 'b' indicate significant and not significant differences between treatments and the control respectively). IR, ionizing radiation.

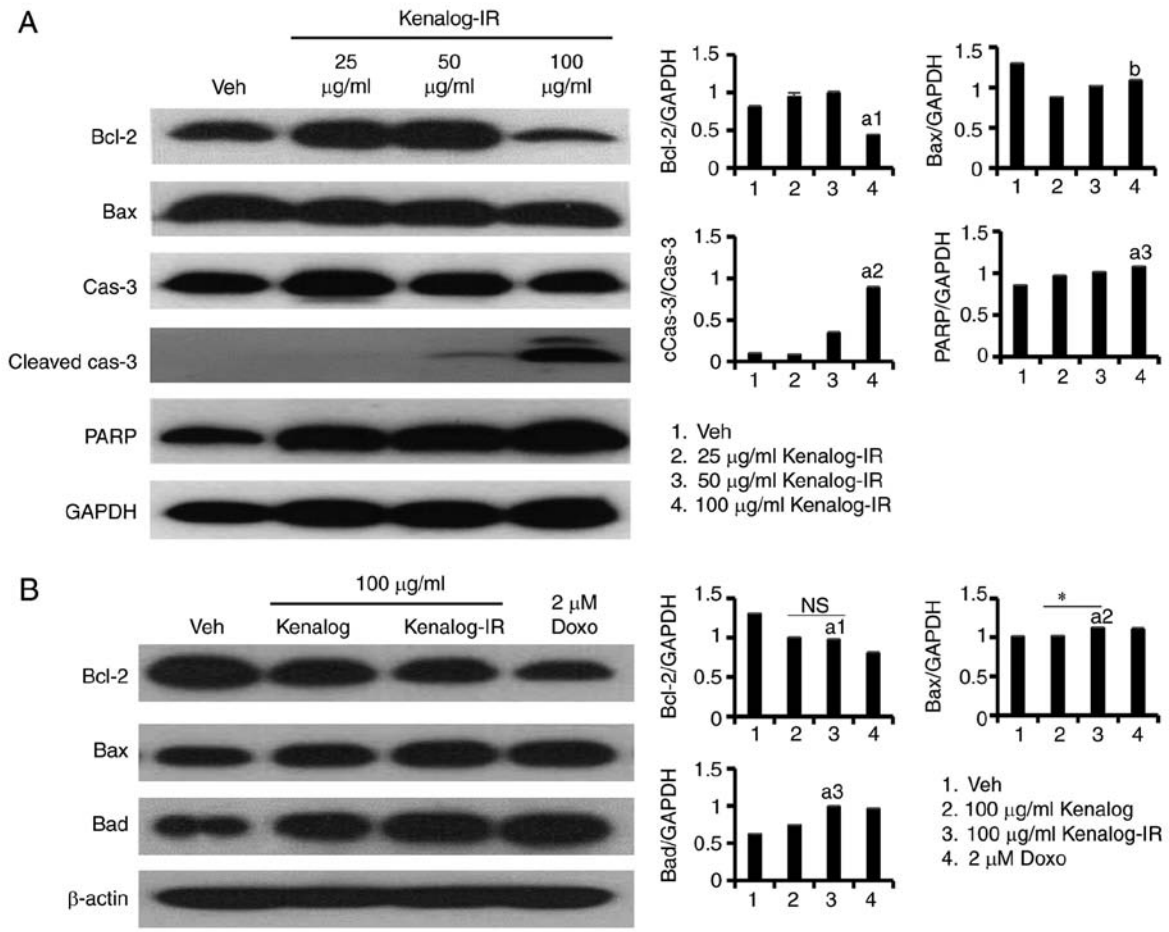

Figure 4. Kenalog-IR induces apoptosis through the intrinsic mitochondrial pathway. Analysis of apoptotic protein markers. Whole cell-lysates were extracted by RIPA and an equal amount of protein was analyzed by western blotting. (A) Dose-dependent expression of Bcl-2 family proteins, caspase-3 and PARP gradually determined at 100 μg/ml of Kenalog-IR treatment (^{a1}=1.2x10^{-7}, ^{a2}=3.4x10^{-12}, ^{a3}=0.0065 and ^{b}=0.072). (B) Analysis of pro- and anti-apoptotic Bcl-2 family proteins 24 h after Kenalog-IR treatment (^{a1}=0.041, ^{a2}=0.0042, ^{a3}=4x10^{-8}, $^{n.s}$=0.18 and *=0.00017).

Executioner caspases, markers of the intrinsic pathway were also found to be activated. Kenalog-IR activated the expression of cleaved caspase-7 (P=2.8x10^{-10}) and cleaved caspase-3 (P=2.4x10^{-11}) while it decreased the expression of both the total and the cleaved form of caspase-9 (Fig. 4C) at 24 h of treatment. The activation of caspase-7 and -3 indicated the involvement of the intrinsic pathway. Furthermore, the mediator of the intrinsic pathway involved in the release of the PARP enzyme was investigated. PARP is involved in the release of mitochondrial proteins such as cytochrome *c* or apoptosis-inducing factor (AIF) and regulates its translocation to the cytoplasm (19). Kenalog-IR decreased AIF protein levels in the mitochondria fraction (Fig. 4E, mitochondria fraction lane 3) and induced the expression of cleaved PARP at 24 h of treatment (Fig. 4D). These results demonstrated that Kenalog-IR induced apoptosis through activation of the intrinsic mitochondrial pathway in SK-Mel-5 cells.

Kenalog-IR increases production of ROS which in turn increases mitochondria-mediated apoptosis. Reactive oxygen species (ROS) is the hallmark of apoptosis and a significant indicator of cells undergoing oxidative stress. Normally, the induction of the intrinsic pathway is linked with the leakage of mitochondrial proteins which pass through the distracted electron transport chain (ETC) and stimulate further production of ROS and executor proteins. Based on our aforementioned results, caspase activation in particular caspase-3 and -7 were regarded as key molecules revealing impaired mitochondrial function (20,21). Given these facts, investigation of whether apoptotic induction was linked with ROS production was performed. Using intracellular detection of superoxide radicals by dihydroethidium (DHE), it was revealed that Kenalog-IR significantly induced 84% (P=3.7x10^{-7}) of ROS positive cells (Fig. 5A, lane 4) compared to 31% (P=0.990) of Kenalog-treated cells (Fig. 5A, lane 3). Furthermore, blocking of ROS by N-acetyl-Cysteine (NAC) revealed a reduction of ROS positive cells to 27% (P=0.06) (Fig. 5A, lane 5). These results indicated that Kenalog-IR-induced apoptosis was mediated by ROS production. It is well known that accumulation of superoxide and other oxidative stress molecules are associated with increased levels of ROS which cause increased expression of the enzyme sodium dismutase (SOD) and subsequently a downstream pathway related to ROS induction (Fig. 5C). To ascertain this, the source of ROS induced by Kenalog-IR was first revealed. The MitoSOX assay results revealed that the majority of ROS were generated from the mitochondria (Fig. 5D). To establish whether the increased levels of apoptosis were related to ROS, western blot analysis

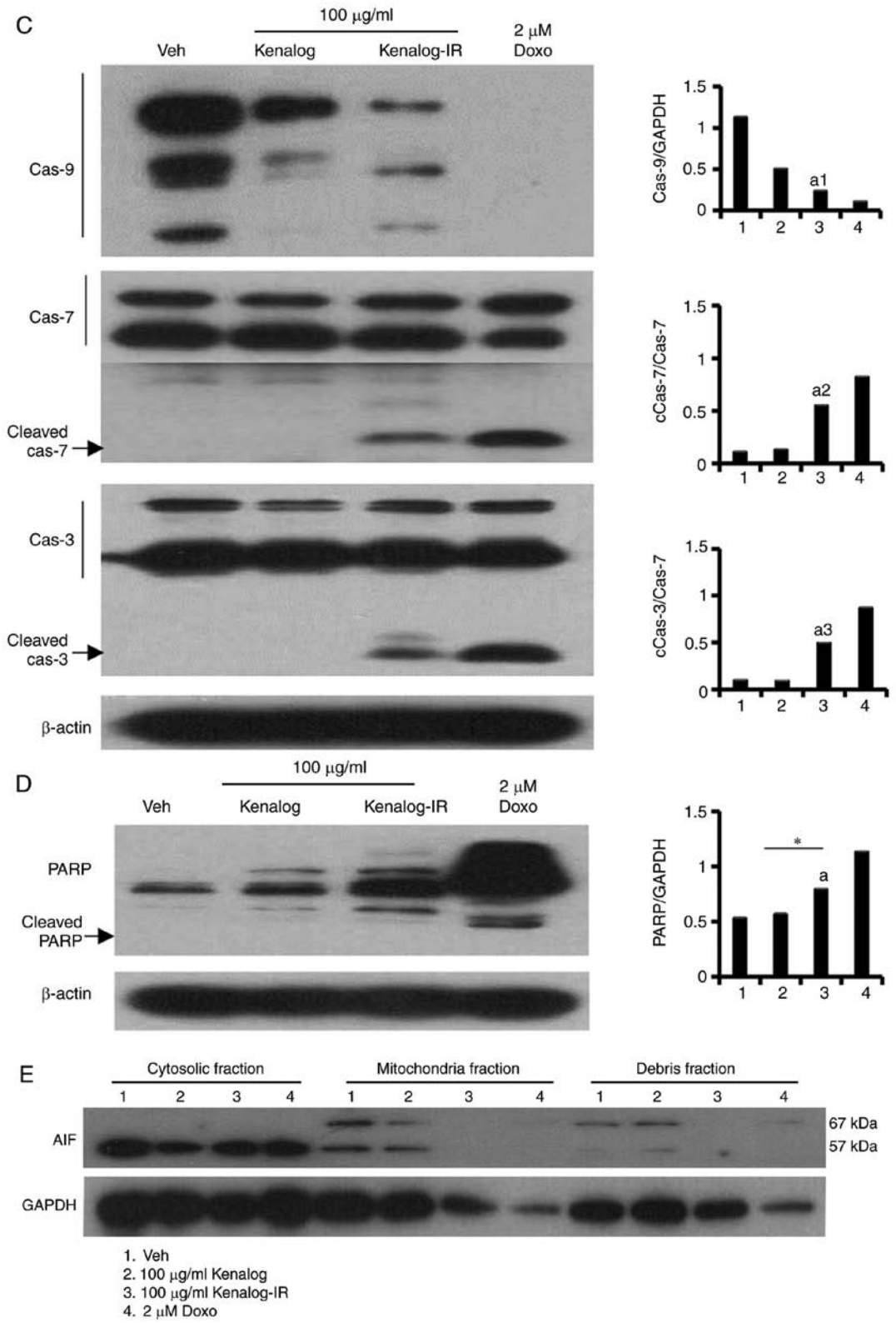

Figure 4. Continued. (C) The Kenalog-IR activated expression of intrinsic apoptosis pathways proteins (^{a1}=1.1x10^{-13}, ^{a2}=2.8x10^{-10} and ^{a3}=2.4x10^{-11}) and (D) Kenalog-IR induced the expression of cleaved PARP 24 h of treatment (^{a}=0.00006 and *=1x10^{-7}). (E) SK-Mel-5 cells were cultured in absence (line 1) or presence of Kenalog (line 2), Kenalog-IR (line 3) and Doxo as a positive control (line 4). Cytosolic and mitochondria fractions were separated by 12% SDS-PAGE. The histograms shown in the right panel of parts A-D indicate ImageJ extracted intensities as normalized against the control protein (GAPDH) or the total form of respective proteins. Data are presented as the mean ± SEM of three independent experiments [*P<0.05 between treatment groups, 'NS' indicates not significant between treatment groups, a small letter 'a' indicates significant differences between treatments and the control or calibrator (GAPDH) or the total form of the protein of interest]. IR, ionizing radiation; Doxo, doxorubicin.

was performed for the ROS-related pathway. The results revealed that the expression level SOD1 was increased in Kenalog-IR-treated cells (Fig. 5E, lane 3) demonstrating that ROS was increased and scavenged by this enzyme.

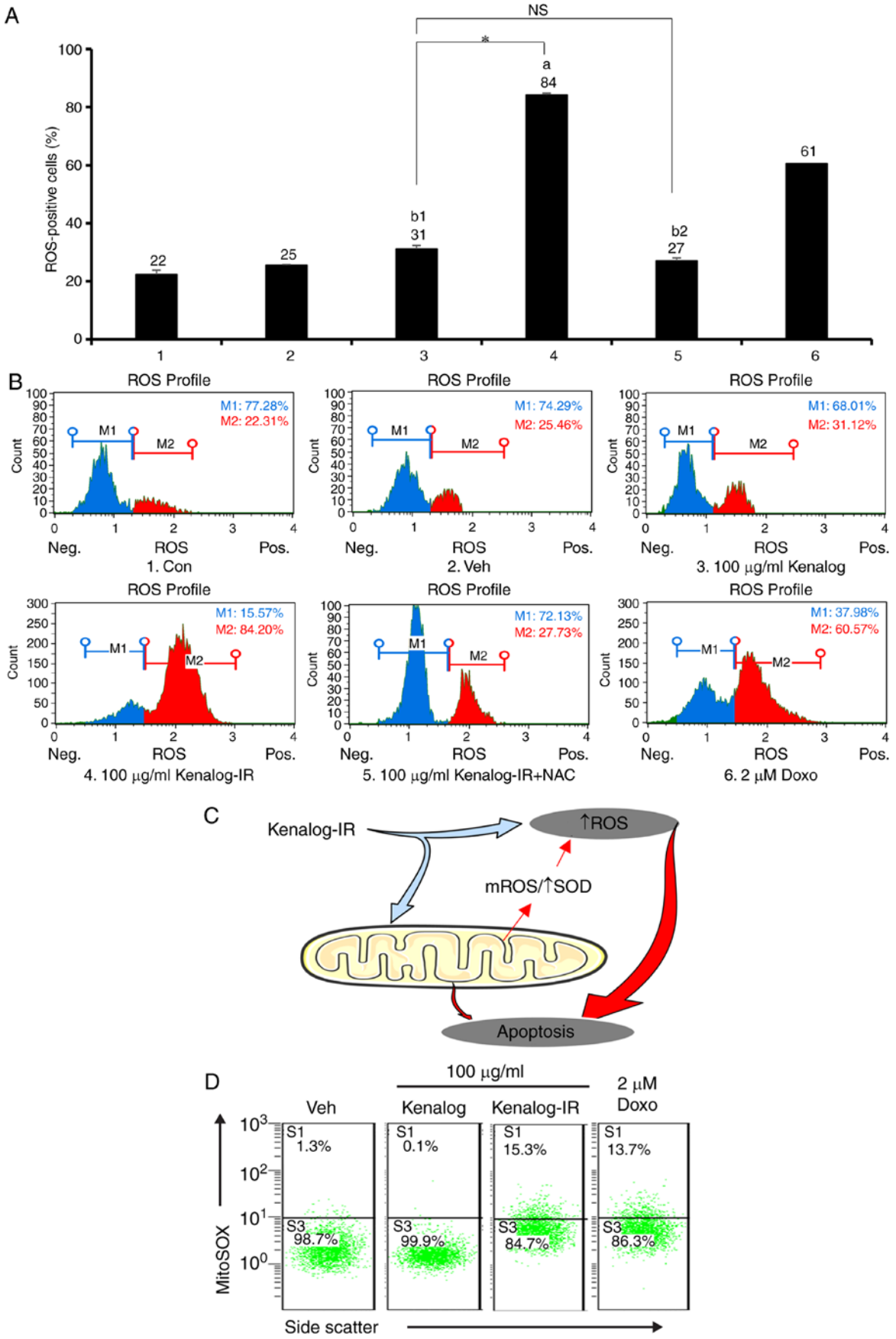

Figure 5. Kenalog-IR increases production of ROS which in turn increases mitochondria-mediated apoptosis. Intracellular ROS levels of SK-Mel-5 cells. Cells treated with Kenalog and Kenalog-IR for 24 h were assessed by flow cytometer. (A) The ROS-negative (M1) and ROS-positive (M2) cells were expressed as a percentage in M1 and M2 gates respectively (^{a}=3.7x10^{-7}, ^{b1}=0.99, ^{b2}=0.06^{5}, *=2.9x10^{-9}, $^{n.s}$=0.175). (B) The population of positive ROS-stained cells was used to calculate the percentage of ROS-stained cells as shown in the histogram. (C) Hypothetical illustration of Kenalog-IR-induced ROS. (D) Mitochondrial ROS determination by flow cytometer. Cells were pre-labeled with 5 μM MitoSOX reagent for 1 h and exposed to treatment for 18 h. Cells were harvested, washed and further incubated with MitoSOX reagent for 10 min at 37˚C in the dark. Quadrants indicate ROS-positive cells.

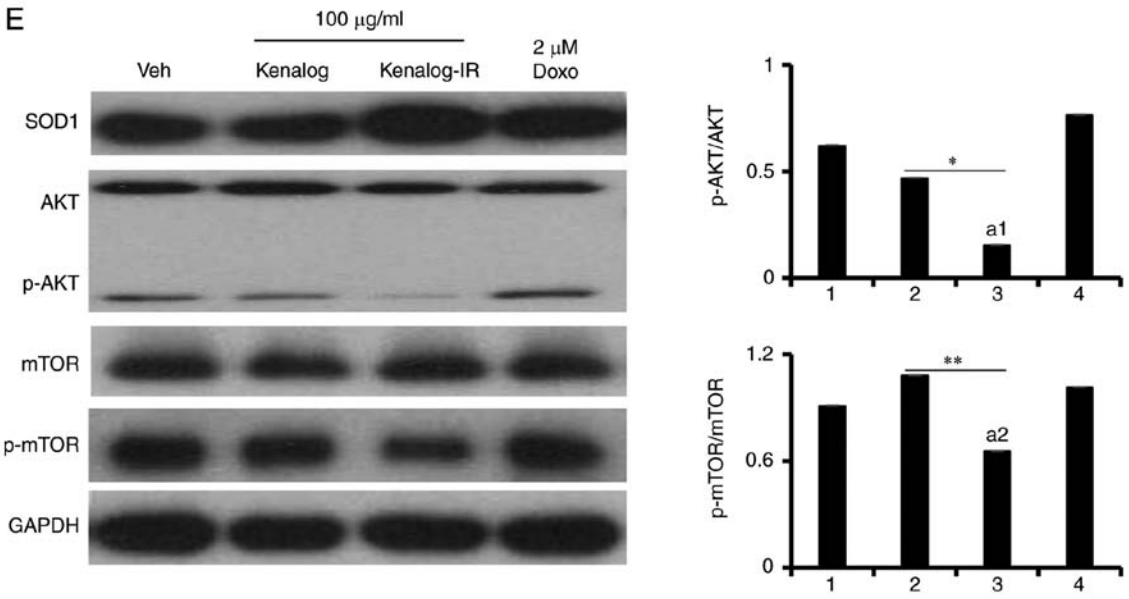

Figure 5. Continued. (E) Analysis of the ROS-mediated pathway. Cells were treated with Kenalog or Kenalog-IR and cell lysates were subjected to 10 or 15% SDS-PAGE. SOD1 was used to denote increased levels of ROS while GAPDH was used as a control. The histograms shown in the right panel indicate ImageJ extracted intensities as normalized against the total protein (^{a1}=2.86x10^{-9}, ^{a2}=2x10^{-5}, *=1.04x10^{-8}, **=0.002). Data are presented as the mean ± SEM of three independent experiments (*P<0.05 between treatment groups, 'NS' indicates not significant between treatment groups, small letters 'a' and 'b' indicate significant and not significant differences between treatments and the control respectively). IR, ionizing radiation; ROS, reactive oxygen species.

Furthermore, decreased expression of both phosphorylated AKT (P=2.86x10^{-9}) and phosphorylated mTOR (P=2x10^{-5}) molecules (Fig. 5E) was observed indicating the involvement of the AKT/mTOR pathway in the induction of apoptosis. The experiments in Fig. 5, revealed that ROS production was the source of Kenalog-IR-induced apoptosis in SK-Mel-5 cells.

Discussion

Kenalog is a synthetic glucocorticoid used to treat various cancers and skin diseases. Treatment with Kenalog rarely achieves sustainable results for patients and has adverse effects. To improve its efficacy, ionizing radiation was used to modify the structure of Kenalog to develop a potential anticancer drug. As analyzed by LC-MS, Kenalog-IR formed four peaks (Fig. 1, lower panel) which indicated a promising role of IR in the field of IMD. While the single structures of Kenalog-IR remain to be isolated, its enhanced anticancer activity cannot be ruled out especially in the treatment of melanoma skin cancer. Previously, research by our group revealed the role of IR in enhancing the activity of anticancer drugs in the treatment of hepatic and lung cancer cells (16,17). The findings of these two studies proposed the innovative use of IR to modify the active structure of various glucocorticoids such as Kenalog to increase their potency. While some studies have revealed the use of Kenalog in the management of ocular inflammatory (7) and choroidal melanoma (6), its effectiveness is constantly challenged like many other glucocorticoids (6,22,23). Furthermore, the biogenesis of melanocytes that produce several intermediate proteins which are highly immunogenic and the ability of skin to produce glucocorticoids from cholesterol limit therapeutic use of several glucocorticoids in skin cancer applications (24). However, in the present study, the enhanced role of Kenalog by IR was reported to improve anticancer activities in melanoma cancer cells.

Generation of apoptosis and apoptosis-related markers in drug treatment trials is a superlative approach in cancer treatment. Apoptosis is an important phenomenon in the mechanism of homeostasis, it balances several processes including cell division and cell demise (25,26). Activation of the apoptosis pathway can be initiated from different entry points, either at the plasma membrane upon death receptor activation (receptor/extrinsic pathway) or at the mitochondria (mitochondrial/intrinsic pathway) (18). While it is generally accepted that the downstream key molecule for the extrinsic pathway is caspase-8, the intrinsic pathway has several key molecules that initiate a cytochrome *c*/Apaf-1/caspase-9-containing apoptosome complex to form a unique network of intrinsic apoptosis (27). The present study, proposed a new modified Kenalog compound, Kenalog-IR which induced characteristic intrinsic apoptosis cell death as observed by suspended apoptotic bodies and plasma membrane protrusion (Fig. 2D) with induction of 62% of total apoptosis (Fig. 3). The results were further confirmed by observed DNA fragmentation (Fig. 3E) in the Kenalog-IR-treated group and the activation of cleaved caspases indicated the involvement of the intrinsic pathway (Figs. 3C, 4E and 5A). The control and regulation of cancer cell death through the intrinsic apoptotic pathway involved induction of protein markers including the release of cytochrome *c* as a result of an imbalance between Bcl-2 family proteins (21,28). The imbalance between these proteins caused the release of caspase proteins from cleaved caspase-9 downstream to cleaved-caspase-3 which was associated with impaired mitochondria, the critical site of ROS production. Manifestation of impaired mitochondria was revealed by an excessive imbalance of Bcl-2 family proteins as observed in Fig. 4A and B, and increased production of

mROS observed in Fig. 5D following Kenalog-IR treatment. Furthermore, the use of antioxidant NAC (Fig. 5A and B) indicated that ROS was the main cause of Kenalog-IR-induced apoptosis associated with intrinsic cell death in melanoma cancer cells. Elevated levels of ROS further triggered the release of intrinsic mitochondrial proteins to the cytosol with subsequent activation of cleaved forms of caspase-7 and -3 and deactivation of cleaved caspase-9 (Fig. 4C) possibly causing the programmed death of melanoma cancer cells (29).

However, initiation and execution of apoptosis are mediated by cysteine-dependent aspartate such as caspase-3 in association with the activation of cleaved poly(ADP-ribose) polymerase PARP (30-32). The PARP enzyme is important in the release of mitochondrial proteins and a crucial molecule in the intrinsic apoptosis pathway (30). Attenuation of AIF in the mitochondria fraction (Fig. 4E) and increased levels of cleaved PARP observed in Fig. 4D indicated the regulatory role of PARP in the translocation of mitochondrial proteins involved in programmed cell death. To relate the mechanism of intrinsic apoptosis with the ROS-mediated cell death induced by Kenalog-IR, increased G2/M phase cell arrest was observed even when the cells were treated with nocodazole a known inducer of G2/M cell arrest. This observation indicated that Kenalog-IR affected the cell cycle associated with ROS through the AKT/mTOR signaling pathway (Fig. 5D). The PI3K/AKT/mTOR pathway plays an important role in cell proliferation, migration, cellular metabolism, protein synthesis and apoptosis (33). Phosphorylated AKT (p-AKT) activates many downstream targets including mTOR and GSK-3β, which are important in controlling the cell cycle and apoptosis (34). Since, Kenalog-IR attenuated phosphorylation of AKT and mTOR in SK-Mel-5 cells, this may indicate that cell death involved with cell cycle progression and proliferation may also induce cell death.

Collectively, the findings of the present study elucidated the mechanism of cell death induced by Kenalog-IR during melanoma cancer treatment, however the use of such a therapeutic approach especially in skin cancers still remains challenging. Several corticosteroids and glucocorticoids have been reported to have low solubility, low bioavailability and longer duration of action (12). The increased cytotoxic effect of Kenalog-IR may suggest improved bioavailability and shortened duration of action in melanoma cells when compared to Kenalog (Fig. 2). Since many glucocorticoids are immunosuppressive, we suggested that the actions induced by Kenalog-IR may be attributed to commonly known transcriptional effects of glucocorticoid receptor (GR) agonists which alter the transcription of many genes involved in cell death. This may lead to increased binding affinity of GR(s), known to be G2/M cell-cycle dependent (Fig. 3G), which partly enhanced cellular death by Kenalog-IR (35,36). This may also indicate that intrinsic apoptosis is not the only mechanism of cell death induced by Kenalog-IR, instead other glucocorticoid-induced signaling pathways may lead to cell death. Furthermore, due to the biogenesis of melanocytes (24), the cytotoxic effects induced to the surrounding environment by both melanoma cells and the drug remain a challenge which requires a resolution.

In conclusion, the present study, elucidated the importance of an IR-modified drug in cancer treatment. Kenalog-IR inhibited melanoma cancer cell proliferation and caused cell death by the intrinsic apoptosis pathway. Moreover, Kenalog-IR-induced cell death was associated with increased production of ROS modulated by the release of caspases and activation of cleaved PARP. In general, the results of the present study, justify the hypothesis that incrementally modified drugs by IR may potentially be used as anticancer candidates in various cancer treatment strategies. However, further studies will have to be conducted in the future to determine the structures of Kenalog generated by IR and the stability of these compounds before being subjected to clinical trials.

Acknowledgements

Not applicable.

Funding

This research was funded by the Ministry of Science and ICT through the Basic Science Research Program by the Korean government.

Availability of data and materials

The analyzed datasets generated during the study are available from the corresponding author upon reasonable request.

Authors' contributions

RAK, EHL and HWB conceived, designed and wrote the study. RAK, FJR, HJC and CHP performed the experiments and analyzed data. BYC and HWB were involved in the conception of the study, supervised the experimental work and revised the manuscript. All authors read and approved the manuscript and agree to be accountable for all aspects of the research in ensuring that the accuracy or integrity of any part of the work are appropriately investigated and resolved.

Ethics approval and consent to participate

Not applicable.

Patients consent for publication

Not applicable.

Competing interests

The authors state that they have no competing interests.

References

1. Haller J, Mikics É and Makara GB: The effects of non-genomic glucocorticoid mechanisms on bodily functions and the central neural system. A critical evaluation of findings. Front Neuroendocrinol 29: 273-291, 2008.
2. Wooldridge JE, Anderson CM and Perry MC: Corticosteroids in advanced cancer. Oncology 15: 225-234, 2001.
3. Kim DW, Kim YI, Ud Din F, Cho KH, Kim JO and Choi HG: Development of a novel triamcinolone acetonide-loaded spray solution for the treatment of stomatitis. Pharmazie 69: 512-517, 2014.

4. Paspulati A, Punjabi OS, Theodoropoulou S and Singh RP: Triamcinolone acetonide as an adjuvant to membrane peeling surgery: A pilot study. Ophthalmic Surg, Lasers Imaging Retina 44: 41-45, 2013.
5. Takata S, Masuda T, Nakamura S, Kuchimaru T, Tsuruma K, Shimazawa M, Nagasawa H, Kizaka-Kondoh S and Hara H: The effect of triamcinolone acetonide on laser-induced choroidal neovascularization in mice using a hypoxia visualization bio-imaging probe. Sci Rep 5: 9898, 2015.
6. Shields CL, Demirci H, Dai V, Marr BP, Mashayekhi A, Materin MA, Manquez ME and Shields JA: Intravitreal triamcinolone acetonide for radiation maculopathy after plaque radiotherapy for choroidal melanoma. Retina 25: 868-874, 2005.
7. Yeung CK, Chan KP, Chan CK, Pang CP and Lam DS: Cytotoxicity of triamcinolone on cultured human retinal pigment epithelial cells: Comparison with dexamethasone and hydrocortisone. Jap J Ophthalmol 48: 236-242, 2004.
8. Perretti M, Paul-Clark M, Mancini L and Flower R: Generation of innovative anti-inflammatory and anti-arthritic glucocorticoid derivatives that release NO: The nitro-steroids. Dig Liver Dis 35: S41-S48, 2003.
9. Wyles CC, Houdek MT, Wyles SP, Wagner ER, Behfar A and Sierra RJ: Differential cytotoxicity of corticosteroids on human mesenchymal stem cells. Clin Orthop Relat Res 473: 1155-1164, 2015.
10. Slominski A, Gomez-Sanchez CE, Foecking MF and Wortsman J: Metabolism of progesterone to DOC, corticosterone and 18OHDOC in cultured human melanoma cells. FEBS Lett 455: 364-366, 1999.
11. Slominski A, Zjawiony J, Wortsman J, Semak I, Stewart J, Pisarchik A, Sweatman T, Marcos J, Dunbar C and C Tuckey R: A novel pathway for sequential transformation of 7-dehydrocholesterol and expression of the P450scc system in mammalian skin. Eur J Biochem 271: 4178-4188, 2004.
12. Henderson NK and Sambrook PN: Relationship between osteoporosis and arthritis and effect of corticosteroids and other drugs on bone. Curr Opin Rheumatol 8: 365-369, 1996.
13. Ha D, Choi Y, Kim DU, Chung KH and Lee EK: A comparative analysis of the impact of a positive list system on new chemical entity drugs and incrementally modified drugs in South Korea. Clin Ther 33: 926-932, 2011.
14. Paul-Clark M, Del Soldato P, Fiorucci S, Flower RJ and Perretti M: 21-NO-prednisolone is a novel nitric oxide-releasing derivative of prednisolone with enhanced anti-inflammatory properties. Br J Pharmacol 131: 1345-1354, 2000.
15. Guo Z, Guo A, Guo Q, Rui M, Zhao Y, Zhang H and Zhu S: Decomposition of dexamethasone by gamma irradiation: kinetics, degradation mechanisms and impact on algae growth. Chemical Engineering J 307: 722-728, 2017.
16. Badaboina S, Bai HW, Na YH, Park CH, Kim TH, Lee TH and Chung BY: Novel radiolytic rotenone derivative, rotenoisin B with potent anti-carcinogenic activity in hepatic cancer cells. Int J Mol Sci 16: 16806-16815, 2015.
17. Lee EH, Park CH, Choi HJ, Kawala RA, Bai HW and Chung BY: Dexamethasone modified by gamma-irradiation as a novel anticancer drug in human non-small cell lung cancer. PLoS One 13: e0194341, 2018.
18. Elmore S: Apoptosis: A review of programmed cell death. Toxicol Pathol 35: 495-516, 2007.
19. Seong YA, Shin PG and Kim GD: Anacardic acid induces mitochondrial-mediated apoptosis in the A549 human lung adenocarcinoma cells. Int J Oncol 42: 1045-1051, 2013.
20. Cai J, Yang J and Jones DP: Mitochondrial control of apoptosis: The role of cytochrome *c*. Biochim Biophys Acta 1366: 139-149, 1998.
21. Wu CC and Bratton SB: Regulation of the intrinsic apoptosis pathway by reactive oxygen species. Antioxid Redox Signal 19: 546-558, 2013.
22. el Filali M, Homminga I, Maat W, van der Velden PA and Jager MJ: Triamcinolone acetonide and anecortave acetate do not stimulate uveal melanoma cell growth. Mol Vis 14: 1752-1759, 2008.
23. Gao H, Qiao X, Gao R, Mieler WF, McPherson AR and Holz ER: Intravitreal triamcinolone does not alter basal vascular endothelial growth factor mRNA expression in rat retina. Vision Res 44: 349-356, 2004.
24. Slominski AT and Carlson JA: Melanoma resistance: A bright future for academicians and a challenge for patient advocates. Mayo Clin Proc 429-433, 2014.
25. Cheng YL, Lee SC, Lin SZ, Chang WL, Chen YL, Tsai NM, Liu YC, Tzao C, Yu DS and Harn HJ: Anti-proliferative activity of *Bupleurum scrozonerifolium* in A549 human lung cancer cells in vitro and in vivo. Cancer Lett 222: 183-193, 2005.
26. Ye YT, Zhong W, Sun P, Wang D, Wang C, Hu LM and Qian JQ: Apoptosis induced by the methanol extract of *Salvia miltiorrhiza Bunge* in non-small cell lung cancer through PTEN-mediated inhibition of PI3K/Akt pathway. J Ethnopharmacol 200: 107-116, 2017.
27. Fulda S and Debatin KM: Extrinsic versus intrinsic apoptosis pathways in anticancer chemotherapy. Oncogene 25: 4798, 2006.
28. Ma Y, Zhu B, Yong L, Song C, Liu X, Yu H, Wang P, Liu Z and Liu X: Regulation of intrinsic and extrinsic apoptotic pathways in osteosarcoma cells following oleandrin treatment. Int J Mol Sci 17: E1950, 2016.
29. Kroemer G, Galluzzi L and Brenner C: Mitochondrial membrane permeabilization in cell death. Phys Rev 87: 99-163, 2007.
30. Cregan SP, Dawson VL and Slack RS: Role of AIF in caspase-dependent and caspase-independent cell death. Oncogene 23: 2785-2796, 2004.
31. Hwang JT, Kwak DW, Lin SK, Kim HM, Kim YM and Park OJ: Resveratrol induces apoptosis in chemoresistant cancer cells via modulation of AMPK signaling pathway. Ann NY Acad Sci 1095: 441-448, 2007.
32. Hwang JT, Ha J, Park IJ, Lee SK, Baik HW, Kim YM and Park OJ: Apoptotic effect of EGCG in HT-29 colon cancer cells via AMPK signal pathway. Cancer Lett 247: 115-121, 2007.
33. Morgensztern D and McLeod HL: PI3K/Akt/mTOR pathway as a target for cancer therapy. Anticancer Drugs 16: 797-803, 2005.
34. Dobbin ZC and Landen CN: The importance of the PI3K/AKT/MTOR pathway in the progression of ovarian cancer. Int J Mol Sci 14: 8213-8227, 2013.
35. Ashwell JD, Lu FW and Vacchio MS: Glucocorticoids in T cell development and function. Ann Rev Immunol 18: 309-345, 2000.
36. Coutinho AE and Chapman KE: The anti-inflammatory and immunosuppressive effects of glucocorticoids, recent developments and mechanistic insights. Mol Cell Endocrinol 335: 2-13, 2011.